analytical chemistry

pubs.acs.org/ac

Article

Multiplexed Lab-on-a-Chip Bioassays for Testing Antibodies against SARS-CoV-2 and Its Variants in Multiple Individuals

Lei Mou,[‖] Yingying Zhang,[‖] Yao Feng, Honghai Hong, Yong Xia,* and Xingyu Jiang*

Cite This: *Anal. Chem.* 2022, 94, 2510−2516

Read Online

ACCESS | Metrics & More | Article Recommendations | Supporting Information

ABSTRACT: Neutralization assays that can measure neutralizing antibodies in serum are vital for large-scale serodiagnosis and vaccine evaluation. Here, we establish multiplexed lab-on-a-chip bioassays for testing antibodies against severe acute respiratory syndrome coronavirus 2 (SARS-CoV-2) and its variants. Compared with enzyme-linked immunosorbent assay (ELISA), our method exhibits a low consumption of sample and reagents (10 μL), a low limit of detection (LOD: 0.08 ng/mL), a quick sample-to-answer time (about 70 min), and multiplexed ability (5 targets in each of 7 samples in one assay). We can also increase the throughput as needed. The concentrations of antibodies against RBD, D614G, N501Y, E484K, and L452R/E484Q-mutants after two doses of vaccines are 6.6 ± 3.6, 8.7 ± 4.6, 3.4 ± 2.8, 3.8 ± 2.8, and 2.8 ± 2.3 ng/mL, respectively. This suggests that neutralizing activities against N501Y, E484K, and L452R/E484Q-mutants were less effective than RBD and D614G-mutant. We performed a plaque reduction neutralization test (PRNT) for all volunteers. Compared with PRNT, our assay is fast, accurate, inexpensive, and multiplexed with multiple-sample processing ability, which is good for large-scale serodiagnosis and vaccine evaluation.

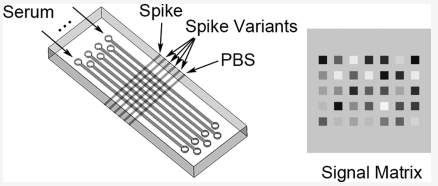

INTRODUCTION

The ongoing coronavirus disease 2019 (COVID-19) pandemic, caused by severe acute respiratory syndrome coronavirus 2 (SARS-CoV-2), is still a major public safety issue worldwide. Meanwhile, SARS-CoV-2 has many variants. The U.K. variant B.1.1.7, the Brazil variant P.1, the South Africa variant B.1.351, and the most recent India variant B.1.617 are of particular concern because of their high prevalence.[1,2] Large-scale vaccination and sensitive detection are vital for preventing the spread of the COVID-19 pandemic.[3−9] Virus neutralization assays that can measure neutralizing antibodies in serum are vital for determining vaccine efficacy.[10] Recent studies show that antibodies that target the receptor-binding domain (RBD) of spike protein are strong indicators of the effectiveness of vaccines.[11−14] However, not all antibodies binding to SARS-CoV-2 spike protein block the activity of virus. Enzyme-linked immunosorbent assay (ELISA) for antibody detection shows a good correlation with the neutralizing activity.[15] This kind of assay can also promote the COVID-19 serodiagnosis, the evaluation of recombinant therapeutic antibodies, vaccine verification, and vaccine development.[16−18]

An ideal neutralizing antibody assay should be fast, accurate, inexpensive, and multiplexed with multiple-sample processing ability. The gold standard to determine virus neutralization efficacy after vaccination is the plaque reduction neutralization test (PRNT).[2,19] Traditional PRNT can be optimized using fluorescence-based neutralization assay or pseudotyped virus-based assay.[10,20,21] However, these assays are still lab-intensive, time-consuming, and need to be performed at biosafety level 3. These disadvantages hinder their application in large-scale serodiagnosis and vaccine evaluation. The use of multiplexed immunoassay for testing SARS-CoV-2 and its variants is highly needed.[5,22,23] Microfluidic chip has provided a versatile platform for developing a multiplexed immunoassay with a lower consumption of sample and reagents, a lower limit of detection (LOD), and a quicker sample-to-answer time than conventional ELISA.[4,24−32]

Inspired by the microarray immunoassay for the simultaneous detection of proteins,[33,34] here, we report multiplexed lab-on-a-chip bioassays for testing antibodies against SARS-CoV-2 and its variants. Thirty-five volunteers who received vaccines were involved in our experiment. Three serum samples of each volunteer were collected (Figure 1a; Serum 1: before the first injection of vaccine, Serum 2: 2 weeks after the first injection of vaccine, Serum 3: 2 weeks after the second injection of vaccine). The RBDs of SARS-CoV-2 spike protein and its variants (E484K, N501Y, D614G, and L452R/E484Q-mutants) were used as an ELISA antigen to enhance the specificity of our assay (Figure 1b). These variants are present in U.K., Brazil, South Africa, and India variants. The principle of our assay is illustrated in Figure 1c. To enhance the throughput, we performed the immunoassay on our seven-channel chip (Figure S1). Spike RBD and its variants were first

Received: October 8, 2021
Accepted: January 17, 2022
Published: January 26, 2022

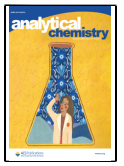

https://doi.org/10.1021/acs.analchem.1c04383
Anal. Chem. 2022, 94, 2510−2516

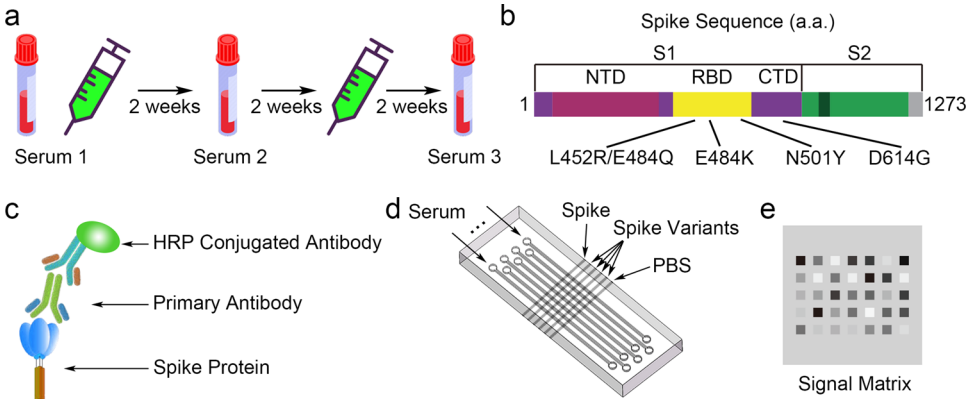

Figure 1. Schematic illustration of the multiplexed lab-on-a-chip bioassays for testing antibodies against SARS-CoV-2 and its variants. (a) Serum samples were collected before and after the injection of vaccines. The serum samples were named by serum 1, serum 2, and serum 3. (b) SARS-CoV-2 spike protein sequence and its variants. The receptor-binding domains (RBDs) of SARS-CoV-2 spike protein and its variants (E484K, N501Y, D614G, and L452R/E484Q-mutants) were used as an ELISA antigen to enhance the specificity of our assay. (c) Principle of chemiluminescence immunoassay. (d) Detect multiple biomarkers in multiple samples with the seven-channel chip. (e) The concentration of antibodies was analyzed through the signal matrix.

patterned on a membrane using the seven-channel chip. After washing, a new seven-channel chip was assembled perpendicular to the previous one resulting in multiple reaction sites. Different serum samples were injected into different channels. In this situation, we can perform immunoassays that detect multiple biomarkers in multiple samples (Figure 1d). Our assay has advantages in handling multiple samples and multiple biomarkers in one assay. Each test can detect six targets (RBD, D614G, N501Y, E484K, L452R/E484Q-mutants, and 1 blank) of seven samples. The concentration of antibodies was analyzed through the signal matrix (Figure 1e). Collectively, our assay can perform multiplexed immunoassay for testing antibodies against SARS-CoV-2 and its variants with a lower consumption of sample and reagents, a lower limit of detection (LOD), and a quicker sample-to-answer time than conventional ELISA.

EXPERIMENTAL SECTION

Materials and Devices. Phosphate-buffered saline (PBS) is from Sangon Biotech (Shanghai). Tween 20 is from Amresco. Bovine serum power (BSA) is from Acmec Biochemical (Shanghai). Poly(dimethylsiloxane)s (PDMS) chip is fabricated with SYLGARD184 from Dow Corning. SARS-CoV-2 spike RBD protein (40592-V08H) and their variants (India variant B.1.617: 40592-V08H88; U.K. variant B.1.1.7: 40592-V08H82; South Africa variant B.1.351: 40592-V08H84; Brazil variant P.1: 40591-V08H5) are from Sino Biological (Beijing). SARS-CoV-2 spike antibody is from Sino Biological (Beijing). Horseradish peroxidase (HRP)-labeled anti-human IgG (40R-1008) is from Fitzgerald Industries International. HRP 3,3′,5,5′-tetramethylbenzidine (TMB) substrate is from Thermo Fisher Scientific. The absorbance was measured by a microplate reader (FluoStar Omega, BMG Labtech). Immobilon Western chemiluminescent HRP substrate is from EMD Millipore. The chemiluminescent signal (CL) is captured by our portable device. All photos are captured by a Nikon D90 (Japan).

Blood Sample Processing and Storage. During our experiments, we recruited 35 volunteers who received two doses of vaccines. The experiments were performed according to the ethical guidelines (The Ethics Guidelines for Research Involving Human Subjects or Human Tissue from the Third Affiliated Hospital of Guangzhou Medical University: 2021-001). Whole blood samples were collected at Third Affiliated Hospital of Guangzhou Medical University and processed within 24 h. Serums are obtained by centrifugation. After serums are separated, and all serums are stored at −20 °C before use.

Fabrication of Microfluidic Chip. The microfluidic chip consists of two PDMS layers. The top layer contains seven parallel microchannels for sample introduction (Figure S1), and the bottom layer is immobilized with detection antigens. The seven-channel chip was fabricated by traditional soft lithography. The poly(methyl methacrylate) mold is designed with SolidWorks and fabricated by a local manufacturer company (Shenzhen Yungu Precision Manufacturing Co., Ltd.). Uncured PDMS (prepolymer/curing agent = 10:1) was poured onto the mold and degassed for 10 min. The degassed PDMS was cured in an 80 °C oven for 30 min. The inlets and outlets of the PDMS top layer were punched using a syringe needle with a flattened tip. We use the PDMS membrane as our immunoassay reaction substrate. The seven-channel chip was assembled on the PDMS membrane. The top seven-channel chip was adhered to the bottom PDMS membrane by the hydrophobic interaction.

ELISA. PBS (10 mM, pH 7.4) was used as the baseline buffer. The washing buffer was prepared by dissolving Tween 20 in 10 mM PBS of pH 7.4 (PBST). BSA (0.3 g) was dissolved in 10 mL of PBS of pH 7.4 to prepare 3% BSA as the blocking agent. SARS-CoV-2 spike protein (100 μL, 1 μg/mL) was incubated onto the 96-well plates overnight at 4 °C. The plates were washed three times with PBST washing buffer. BSA blocking buffer (300 μL, 3%) was added to each well for 2 h at room temperature. After removing all reagents, 100 μL of SARS-CoV-2 spike antibodies with different concentrations was added into different wells and incubated for 2 h. The plates were washed three times with washing buffer and then incubated with 100 μL of HRP-labeled anti-human IgG (1000 times of dilution). After washing three times, 100 TMB substrate was added to the plate for 10 min. The reaction was stopped by adding 100 μL of 1 M H_2SO_4. The concentration of spike antibodies was measured by detecting the absorbance at 450 nm.

https://doi.org/10.1021/acs.analchem.1c04383
Anal. Chem. 2022, 94, 2510−2516

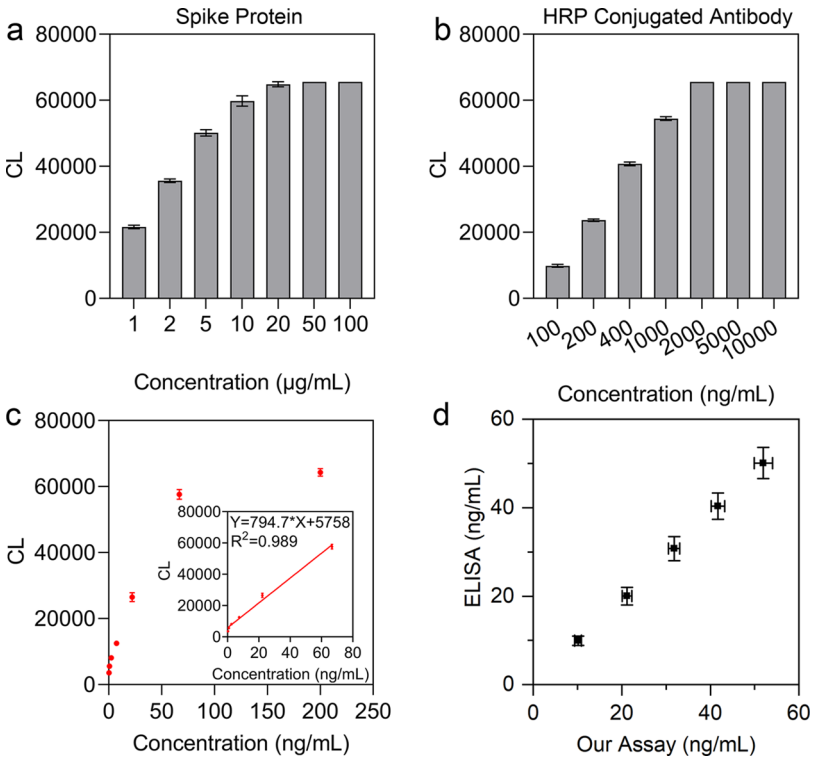

Figure 2. Performance of multiplexed lab-on-a-chip immunoassays. (a) Optimization of the concentration of SARS-CoV-2 spike protein. The CL signal is saturated when the concentration is over 10 μg/mL. (b) Optimization of the concentration of HRP-labeled anti-human IgG. The CL signal is saturated when the concentration is over 1000 ng/mL. For the following experiments, the concentration of SARS-CoV-2 spike protein and HRP-labeled anti-human IgG are 10 and 1000 ng/mL, respectively. (c) Standard curve of our multiplexed lab-on-a-chip immunoassays for detecting antibodies. The standard equation is $Y = 794.7 \times X + 5758$, $R^2 = 0.989$. (d) Comparison of our assay with conventional ELISA. Our assay shows high consistency with ELISA methods. The coefficient of variation of our assay is better than ELISA.

Multiplexed Lab-on-a-Chip Immunoassays. The procedure of multiplexed lab-on-a-chip immunoassays involves six steps (Figure S2). Injections of all reagents and samples are manually done by operating the pipette. As this assay is not yet automated, no external valve and pump are needed. (1) SARS-CoV-2 spike RBD and its variants (10 μg/mL) were introduced into the seven-channel chip. Each channel has one type of SARS-CoV-2 spike protein. Spike RBDs were incubated into the channel for 30 min and patterned onto the PDMS membrane. After 30 min, the channels were washed three times with PBS to remove the unbound antigen. (2) The seven-channel chip was peeled off. A new seven-channel chip adhered to the bottom PDMS membrane perpendicularly to the immobilized antigen strips. 3% BSA was introduced into the seven-channel chip and incubated for 30 min. (3) Different serum samples were added into different channels and incubated for 30 min. The antibodies were detected by the immobilized spike proteins. After 30 min, the channels were washed three times with a PBST washing buffer. (4) HRP-labeled anti-human IgG (100 times dilution) was added into channels and incubated for 30 min. After 30 min, the channels were washed three times with the PBST washing buffer. (5) The seven-channel chip was peeled off. Chemiluminescent substrate (1 mL) was added onto the PDMS membrane. The CL images are captured by a customized CCD camera and software, which has been previously reported.[24,25] Under the optimized condition, the value of captured signal represents the intensity of CL. We can read these values from the software. The concentration of antibodies was calculated based on the CL.

Competitive Immunoassay. Here, we compared our assay with the SARS-CoV-2 inhibitor screening ELISA kit (KIT001, CW15MA2501, Sino Biological). Human ACE2-his (100 μL) and serum samples (100 μL) were added to each well. The 96-plate was precoated with SARS-CoV-2 spike RBD protein. After 1 h, each well was washed three times with a washing buffer. After washing, 100 μL of anti-his tag antibody (HRP) was added to each well and reacted for 1 h. After washing three times, a 100 TMB substrate was added to the plate for 10 min. The reaction was stopped by adding 100 μL of 1 M H_2SO_4. The concentration of antibodies was measured by detecting the absorbance at 450 nm. The signal color becomes lighter as the concentration of SARS-CoV-2 antibody increases.

SARS-CoV-2 Plaque Reduction Neutralization Test. The SARS-CoV-2 plaque reduction neutralization test was performed as a reported protocol.[35] The procedure of PRNT has six steps. (1) The serum was serially diluted with the cell maintenance solution at successive times. (2) Diluted serum (1.0 mL) was added and mixed with 1.0 mL of standard virus (100 $CCID_{50}$) and incubated in a 37 °C water bath for 1 h. (3) The mixed solution (0.2 mL) was added into a 96-well cell culture plate. (4) The virus solution was serially diluted (10 times). The diluted virus solution (0.1 mL) was added to a 96-well cell culture plate. (5) The 96-well cell culture plate was incubated in a 37 °C, 5% CO_2 incubator. (6) The 50% serum neutralization endpoint was calculated by the Reed−Muench method.

Statistical Analysis. All data were analyzed using the software Prism 8 (GraphPad). The standard curve of our assay

https://doi.org/10.1021/acs.analchem.1c04383
Anal. Chem. 2022, 94, 2510−2516

was analyzed by a linear regression model in the software Prism 8. Pearson correlation coefficients are calculated using the default settings in the software Prism 8. Source data are provided with this paper or from the author.

RESULT AND DISCUSSION

Multiplexed Lab-on-a-Chip Immunoassays. The concentrations of SARS-CoV-2 spike protein antigen, HRP-labeled anti-human IgG, and incubation time can affect the detection results. The concentration of SARS-CoV-2 spike protein antigen was optimized from 100 to 1 μg/mL. As expected, the CL increased with increasing concentration of SARS-CoV-2 spike protein antigen. The CL signal is saturated when the concentration is over 10 μg/mL (Figure 2a). We set the concentration of SARS-CoV-2 spike protein antigen as 10 μg/mL in the following experiments. The concentration of HRP-labeled anti-human IgG was optimized from 10 000 to 100 ng/mL. The CL signal is saturated when the concentration is over 1000 ng/mL (Figure 2b). The concentration of HRP-labeled anti-human IgG was 1000 ng/mL in our following experiments. The incubation time of each step was optimized from 10 to 60 min. When the incubation time is over 30 min, there is no significant difference in CL (Figure S3). The incubation time was 30 min in our following experiments. Although the total sample-to-answer time is about 70 min, which is a little bit slower than some flow-based immunoassays,[36−38] our assay can detect multiple biomarkers in multiple individuals (5 targets in each of 7 samples in one assay) in 70 min. The number and samples and targets can be further improved by increasing the number of microfluidic channels.

Table 1. Summarization of the Similarities and Differences between Our Method and ELISA

	ELISA	our assay
LOD	0.57 ng/mL	0.08 ng/mL
time	over 5 h	about 70 min
sample and reagent	100 μL	10 μL
multiplexed	no	yes

After optimization, we produced the standard curve of our multiplexed lab-on-a-chip immunoassays for detection antibodies. The CL increased with the concentration of SARS-CoV-2 spike protein antigen increasing from 200 to 0.27 ng/mL. A strong linear relationship was observed from 66.67 to 0.27 ng/mL with the standard curve of $Y = 794.7 \times X + 5758$, $R^2 = 0.989$ (Figure 2c). The LOD of our assay was determined by the following formula: LOD = $3S/N$ (S: standard deviation of blank sample; N: slope of the standard curve). The LOD of our multiplexed lab-on-a-chip immunoassays is 0.08 ng/mL, which is lower than ELISA (LOD: 0.57 ng/mL, Figure S4). The detection performance comparison was evaluated by

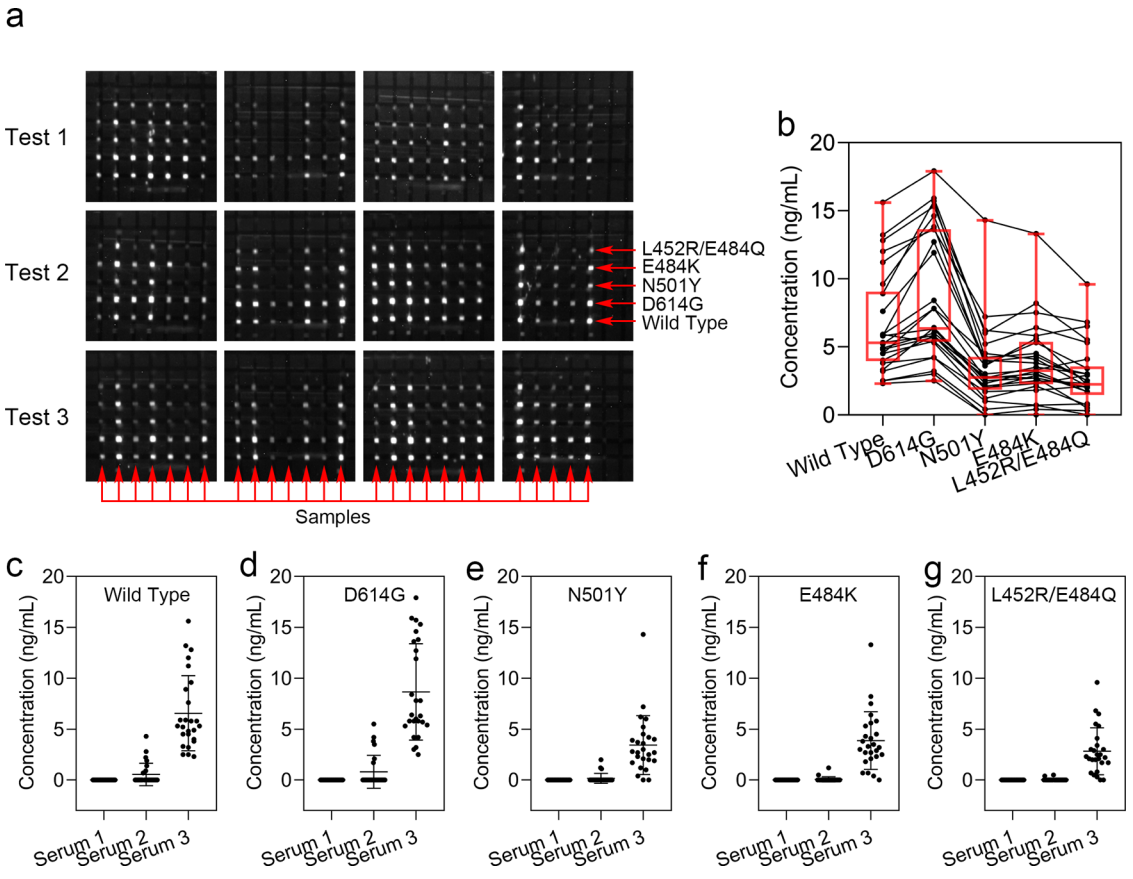

Figure 3. Detection of antibodies with multiplexed lab-on-a-chip immunoassays. (a) Detected signal matrix of serum 3. Each test can detect six targets (RBD, D614G, N501Y, E484K, L452R/E484Q-mutants, and 1 blank) of seven samples. (b) Concentrations of antibodies against RBD, D614G, N501Y, E484K, and L452R/E484Q-mutants. The mean value and standard deviation of each spike protein are inserted. Each line represents a volunteer. (c−g) Concentrations of antibodies against RBD, D614G, N501Y, E484K, and L452R/E484Q-mutants of serum 1, serum 2, and serum 3.

https://doi.org/10.1021/acs.analchem.1c04383
Anal. Chem. 2022, 94, 2510−2516

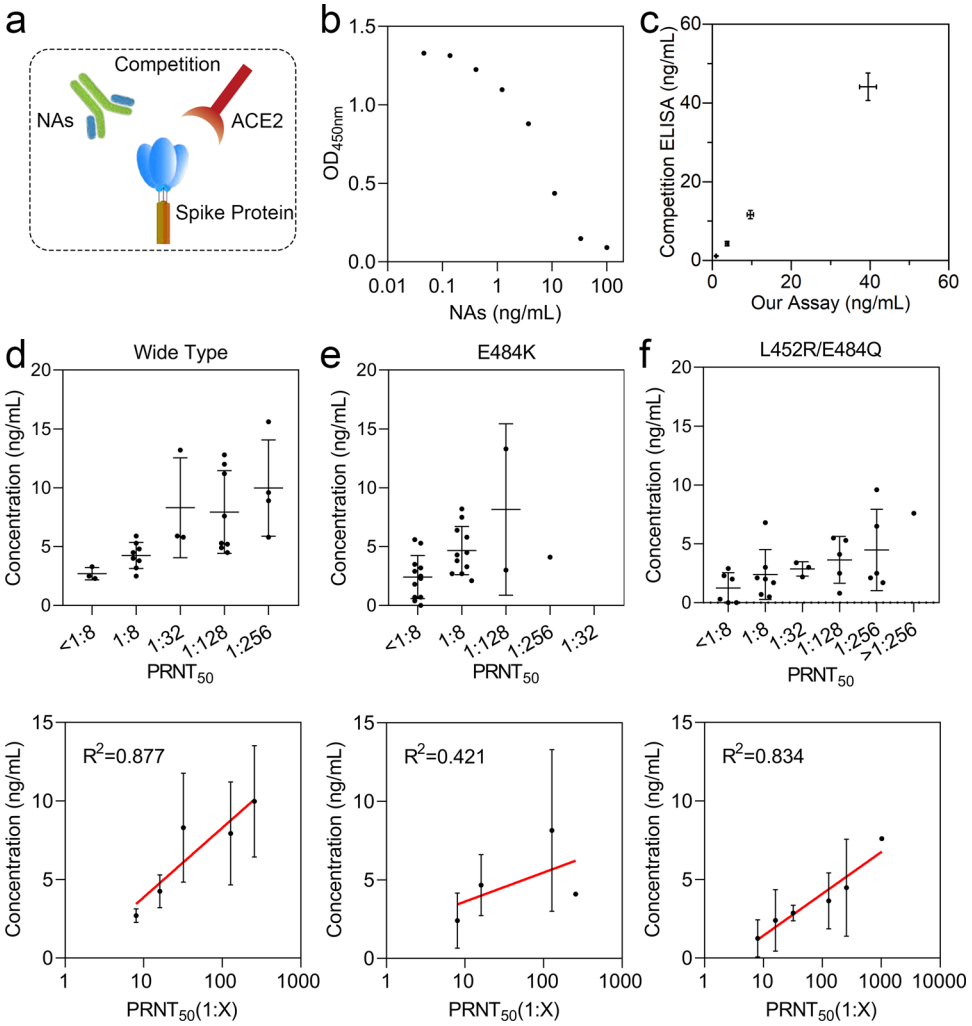

Figure 4. Comparison of our assay with competitive ELISA and PRNT. (a) Schematic illustration of SARS-CoV-2 antibodies competing with ACE2 to combine with SARS-CoV-2 RBD protein. (b) Standard curve of competitive ELISA kit for SARS-CoV-2 antibody. (c) Comparison of our assay with competitive ELISA. Our assay shows high consistency with competitive ELISA methods. (d) Comparison of our assay with PRNT with wild-type viruses, (e) B.1.351 variants, and (f) B.1.617 variants. When we set the dilution times as the *x*-axis and the concentration as the *y*-axis, a good linear relationship can be observed. The R^2 for wild-type viruses, B.1.351 variants, and B.1.617 variants are 0.877, 0.421, and 0.834, respectively.

standard ELISA. We tested five blank serum samples with added antibodies. The concentrations of antibodies were 50−10 ng/mL. Our assay shows good consistency of ELISA for a similar detection principle (Figure 2d). Compared with ELISA, our method has a lower coefficient of variation than ELISA. The consumption of sample and reagents of our assay is 10 μL, which is less than that of ELISA (100 μL). This advantage will be more obvious when performing multiplexed immunoassay. Table 1 summarizes the similarity and differences between our method and ELISA.

Detection of Antibodies in Serum. Our assay can perform multiplexed immunoassay for testing antibodies against SARS-CoV-2 and its variants with a lower consumption of sample and reagents, a lower LOD, and a quicker sample-to-answer time than conventional ELISA. After characterizing our platform, we test all serum samples with our multiplexed lab-on-a-chip immunoassays. During our experiment, we recruited 26 volunteers who completed the whole experiment. The detected signal matrix of serum 3 is presented in Figure 3a. Each test can detect six targets (RBD, D614G, N501Y, E484K, L452R/E484Q-mutants, and 1 blank) of seven samples. Only 10 μL of sample and 40 reagents (4 chips) are required to complete the entire test within 2 h. To ensure accuracy, we tested all serum samples three times. The vaccinated volunteers have a high concentration of antibodies, especially for RBD and D614G-mutant spike protein. The concentrations of antibodies for RBD, D614G, N501Y, E484K, and L452R/E484Q-mutants are 6.6 ± 3.6, 8.7 ± 4.6, 3.4 ± 2.8, 3.8 ± 2.8, and 2.8 ± 2.3 ng/mL, respectively (Figure 3b). The concentration of antibodies for the D614G-mutant is the highest compared with other variants. The antibodies against N501Y, E484K, and L452R/E484Q-mutants were less than RBD and D614G-mutant. This suggests that antibodies should be tested again when other variants are arising to ensure sufficient immunity. The concentrations of antibodies vary from person to person (Figure 3b). Higher antibodies against RBD and D614G-mutant show higher antibodies against N501Y, E484K, and L452R/E484Q-mutants.

The concentrations of antibodies against RBD, D614G, N501Y, E484K, and L452R/E484Q-mutants of serum 1, serum 2, and serum 3 were also analyzed by our multiplexed lab-on-a-chip immunoassays. The concentrations of antibodies

https://doi.org/10.1021/acs.analchem.1c04383
Anal. Chem. 2022, 94, 2510−2516

were significantly increased after two doses of vaccines (Figure 3c−3g). Only a single dose of vaccine cannot generate enough antibodies against SARS-CoV-2 and its variants. Meanwhile, those who have detectable antibodies in the first shot tend to have a high concentration after the second shot.

Comparison of Our Assay with Competitive ELISA and PRNT. The SARS-CoV-2 antibodies in the samples compete with angiotensin-converting enzyme 2 (ACE2) to combine with SARS-CoV-2 RBD protein (Figure 4a). Based on this principle, some competitive ELISA kits are developed. The standard curve of the competitive ELISA kit for SARS-CoV-2 antibody is examined (Figure 4b). To compare our assay with competitive immunoassay, we test four samples with the concentration of antibodies 1, 4, 10, and 40 ng/mL. All of these four samples show a high consistency (Figure 4c). As antibodies and ACE2 compete with the precoated SARS-CoV-2 RBD protein, the detected antibodies by competitive ELISA are slightly higher than our assay.

To correlate the concentration and activity of antibodies, we also performed PRNT for all serum 3. PRNT is the gold standard for detecting and measuring neutralizing antibodies that can neutralize viruses. However, this assay is cumbersome, time-intensive, and need to perform at biosafety level 3 labs. The neutralization titer was defined as the highest dilution of serum to reduce the number of plaques by 50% compared to the serum-free virus ($PRNT_{50}$). Wild-type viruses, B.1.351 variants, and B.1.617 variants are used to test the neutralization efficacy. The results show that high $PRNT_{50}$ values tend to have high concentrations of antibody (Figure 4d−f). We use RBD and its variants as ELISA antigens to ensure the accuracy of immunoassay. Some serum samples with a low concentration of antibodies also show a high $PRNT_{50}$ value. The associations between $PRNT_{50}$ and the concentration of antibodies are examined. We set the dilution times as the *x*-axis and the concentration as the *y*-axis, and a good linear relationship can be observed. The R^2 values for wild-type viruses, B.1.351 variants, and B.1.617 variants are 0.877, 0.421, and 0.834, respectively. The positive correlation between neutralization titers and immunoassay is vital for large-scale serodiagnosis and vaccine evaluation.

CONCLUSIONS

In conclusion, this paper reports a multiplexed immunoassay to test antibodies against SARS-CoV-2 and its variants with a lower consumption of sample and reagents, a lower LOD, and a quicker sample-to-answer time than conventional ELISA. The concentrations of antibodies against RBD, D614G, N501Y, E484K, and L452R/E484Q-mutants are measured by our platform. The antibodies against N501Y, E484K, and L452R/E484Q-mutants were less effective than RBD and D614G-mutant. Compared with PRNT, the gold standard test for detecting neutralizing antibodies, our assay is fast, inexpensive, and multiplexed with multiple-sample processing ability. The use of RBD and its variants as ELISA antigens can enhance the accuracy of our assay. Compared with IgG and IgM assay,[12] our correlation is better. PRNT is lab-intensive and time-consuming and needs to be performed at biosafety level 3 labs. The relationship between immunoassay and PRNT is valuable for large-scale serodiagnosis and vaccine evaluation. Nowadays, it is still hard to replace the gold standard. Neutralization of virus is still an extremely complex biological process, not just the binding of antibodies to the target. The advantage of our method is the enhanced specificity using spike protein RBD as an antigen and increased throughput by microfluidic chips. With the increase in vaccination rates and the emergence of various variants, it is of great significance to quickly and effectively evaluate the effectiveness of our vaccines. Our platform provides a good solution to this problem. Our assay can also be used in COVID-19 serodiagnosis, evaluating recombinant therapeutic antibodies, vaccine verification, and vaccine development in the future.

ASSOCIATED CONTENT

Supporting Information

The Supporting Information is available free of charge at https://pubs.acs.org/doi/10.1021/acs.analchem.1c04383.

Additional information about the design of microfluidic chip, illustration of the multiplexed lab-on-a-chip bioassays, and the ELISA assay (PDF)

AUTHOR INFORMATION

Corresponding Authors

Yong Xia − *Department of Clinical Laboratory, Third Affiliated Hospital of Guangzhou Medical University, Guangzhou, Guangdong 510150, P. R. China;* Email: 377695944@qq.com

Xingyu Jiang − *Department of Clinical Laboratory, Third Affiliated Hospital of Guangzhou Medical University, Guangzhou, Guangdong 510150, P. R. China; Department of Biomedical Engineering, Southern University of Science and Technology, Shenzhen, Guangdong 518055, P. R. China;* orcid.org/0000-0002-5008-4703; Email: jiang@sustech.edu.cn

Authors

Lei Mou − *Department of Clinical Laboratory, Third Affiliated Hospital of Guangzhou Medical University, Guangzhou, Guangdong 510150, P. R. China; Department of Biomedical Engineering, Southern University of Science and Technology, Shenzhen, Guangdong 518055, P. R. China;* orcid.org/0000-0003-4601-6991

Yingying Zhang − *Department of Clinical Laboratory, Third Affiliated Hospital of Guangzhou Medical University, Guangzhou, Guangdong 510150, P. R. China; Department of Clinical Laboratory, Bao'an Authentic TCM Therapy Hospital, Shenzhen, Guangdong 518101, P. R. China*

Yao Feng − *Department of Clinical Laboratory, Third Affiliated Hospital of Guangzhou Medical University, Guangzhou, Guangdong 510150, P. R. China*

Honghai Hong − *Department of Clinical Laboratory, Third Affiliated Hospital of Guangzhou Medical University, Guangzhou, Guangdong 510150, P. R. China*

Complete contact information is available at: https://pubs.acs.org/10.1021/acs.analchem.1c04383

Author Contributions

[‖]L.M. and Y.Z. contributed equally to this work. X.J., Y.X., and L.M. designed and completed most experiments and data analysis. Y.Z., Y.F., and L.M. designed and conducted the microfluidic immunoassay, ELISA, and data analysis. Y.F. and H.H. collected all clinical samples. All authors have participated in the preparation and discussion of this manuscript. They also thank SUSTech Core Research Facilities (SCRF) of Southern University of Science and Technology

https://doi.org/10.1021/acs.analchem.1c04383
Anal. Chem. 2022, 94, 2510−2516

(SUSTech). They are grateful to X.J. for his expert technical and administrative assistance thought the whole experiment.

Funding

The authors thank the National Key R&D Program of China (2018YFA0902600, 2017YFA0205901); the National Natural Science Foundation of China (21535001, 81730051, 21761142006); the Department of Education of Guangdong Province (2020KZDZX1169); the Chinese Academy of Sciences (QYZDJ-SSW-SLH039, 121D11KYSB20170026, XDA16020902); Shenzhen Bay Laboratory (SZBL2019062801004); Guangdong Innovative and Entrepreneurial Research Team Program (2019ZT08Y191); Guangzhou Municipal Science and Technology Bureau (202002020085); and Tencent Foundation through the XPLORER PRIZE for financial support.

Notes

The authors declare no competing financial interest.

REFERENCES

(1) Zou, J.; Xie, X.; Fontes-Garfias, C. R.; Swanson, K. A.; Kanevsky, I.; Tompkins, K.; Cutler, M.; Cooper, D.; Dormitzer, P. R.; Shi, P.-Y. *npj Vaccines* **2021**, *6*, No. 44.
(2) Xie, X.; Liu, Y.; Liu, J.; Zhang, X.; Zou, J.; Fontes-Garfias, C. R.; Xia, H.; Swanson, K. A.; Cutler, M.; Cooper, D.; et al. *Nat. Med.* **2021**, *27*, 620−621.
(3) Chen, Y.; Mei, Y.; Jiang, X. *Chem. Sci.* **2021**, *12*, 4455−4462.
(4) Xianyu, Y.; Wu, J.; Chen, Y.; Zheng, W.; Xie, M.; Jiang, X. *Angew. Chem.* **2018**, *130*, 7625−7629.
(5) Hristov, D.; Rijal, H.; Gomez-Marquez, J.; Hamad-Schifferli, K. *Anal. Chem.* **2021**, *93*, 7825−7832.
(6) Sempowski, G. D.; Saunders, K. O.; Acharya, P.; Wiehe, K. J.; Haynes, B. F. *Cell* **2020**, *181*, 1458−1463.
(7) Xiong, H.; Ye, X.; Li, Y.; Qi, J.; Fang, X.; Kong, J. *Anal. Chem.* **2021**, *93*, 4270−4276.
(8) Merkoçi, A.; Li, C.-z.; Lechuga, L. M.; Ozcan, A. *Biosens. Bioelectron.* **2021**, *178*, No. 113046.
(9) Yue, H.; Huang, M.; Tian, T.; Xiong, E.; Zhou, X. *ACS Nano* **2021**, *15*, 7848−7859.
(10) Muruato, A. E.; Fontes-Garfias, C. R.; Ren, P.; Garcia-Blanco, M. A.; Menachery, V. D.; Xie, X.; Shi, P.-Y. *Nat. Commun.* **2020**, *11*, No. 4059.
(11) Khoury, D. S.; Cromer, D.; Reynaldi, A.; Schlub, T. E.; Wheatley, A. K.; Juno, J. A.; Subbarao, K.; Kent, S. J.; Triccas, J. A.; Davenport, M. P. *Nat. Med.* **2021**, *27*, 1205−1211.
(12) Tang, M. S.; Case, J. B.; Franks, C. E.; Chen, R. E.; Anderson, N. W.; Henderson, J. P.; Diamond, M. S.; Gronowski, A. M.; Farnsworth, C. W. *Clin. Chem.* **2020**, *66*, 1538−1547.
(13) Mendrone-Junior, A.; Dinardo, C. L.; Ferreira, S. C.; Nishya, A.; Salles, N. A.; de Almeida Neto, C.; Hamasaki, D. T.; Facincani, T.; de Oliveira Alves, L. B.; Machado, R. R. G.; Araujo, D. B.; Durigon, E. L.; Rocha, V.; Sabino, E. C. *Transfusion* **2021**, *61*, 1181−1190.
(14) Padoan, A.; Bonfante, F.; Pagliari, M.; Bortolami, A.; Negrini, D.; Zuin, S.; Bozzato, D.; Cosma, C.; Sciacovelli, L.; Plebani, M. *EBioMedicine* **2020**, *62*, No. 103101.
(15) Müller, K.; Girl, P.; von Buttlar, H.; Dobler, G.; Wölfel, R. *J. Virol. Methods* **2021**, *292*, No. 114122.
(16) Therrien, C.; Serhir, B.; Bélanger-Collard, M.; Skrzypczak, J.; Shank, D. K.; Renaud, C.; Girouard, J.; Loungnarath, V.; Carrier, M.; Brochu, G.; Tourangeau, F.; Gilfix, B.; Piche, A.; Bazin, R.; Guérin, R.; Lavoie, M.; Martel-Laferrière, V.; Fortin, C.; Benoit, A.; Marcoux, D.; Gauthier, N.; Laumaea, A. M.; Gasser, R.; Finzi, A.; Roger, M.; Tang, Y.-W.; et al. *J. Clin. Microbiol.* **2021**, *59*, No. e02511-20.
(17) Sasisekharan, V.; Pentakota, N.; Jayaraman, A.; Tharakaraman, K.; Wogan, G. N.; Narayanasami, U. *Proc. Natl. Acad. Sci. U.S.A.* **2021**, *118*, No. e2021615118.
(18) Wang, L.; Zhou, T.; Zhang, Y.; Yang, E. S.; Schramm, C. A.; Shi, W.; Pegu, A.; Oloniniyi, O. K.; Henry, A. R.; Darko, S.; Narpala, S. R.; Hatcher, C.; Martinez, D. R.; Tsybovsky, Y.; Phung, E.; Abiona, O. M.; Antia, A.; Cale, E. M.; Chang, L. A.; Choe, M.; Corbett, K. S.; Davis, R. L.; DiPiazza, A. T.; Gordon, I. J.; Helmold Hait, S.; Hermanus, T.; Kgagudi, P.; Laboune, F.; Leung, K.; Liu, T.; Mason, R. D.; Nazzari, A. F.; Novik, L.; O'Connell, S.; O'Dell, S.; Olia, A. S.; Schmidt, S. D.; Stephens, T.; Stringham, C. D.; Talana, C. A.; Teng, I.-T.; Wagner, D. A.; Widge, A. T.; Zhang, B.; Roederer, M.; Ledgerwood, J. E.; Ruckwardt, T. J.; Gaudinski, M. R.; Moore, P. L.; Doria-Rose, N. A.; Baric, R. S.; Graham, B. S.; McDermott, A. B.; Douek, D. C.; Kwong, P. D.; Mascola, J. R.; Sullivan, N. J.; Misasi, J. *Science* **2021**, *373*, No. eabh1766.
(19) Bewley, K. R.; Coombes, N. S.; Gagnon, L.; McInroy, L.; Baker, N.; Shaik, I.; St-Jean, J. R.; St-Amant, N.; Buttigieg, K. R.; Humphries, H. E.; et al. *Nat. Protoc.* **2021**, *16*, 3114−3140.
(20) Zettl, F.; Meister, T. L.; Vollmer, T.; Fischer, B.; Steinmann, J.; Krawczyk, A.; V'kovski, P.; Todt, D.; Steinmann, E.; Pfaender, S.; et al. *Vaccines* **2020**, *8*, No. 386.
(21) Nie, J.; Li, Q.; Wu, J.; Zhao, C.; Hao, H.; Liu, H.; Zhang, L.; Nie, L.; Qin, H.; Wang, M.; et al. *Nat. Protoc.* **2020**, *15*, 3699−3715.
(22) Zhang, R.; Wu, J.; Ao, H.; Fu, J.; Qiao, B.; Wu, Q.; Ju, H. *Anal. Chem.* **2021**, *93*, 9933−9938.
(23) Jiang, H.-w.; Li, Y.; Zhang, H.-n.; Wang, W.; Yang, X.; Qi, H.; Li, H.; Men, D.; Zhou, J.; Tao, S.-c. *Nat. Commun.* **2020**, *11*, No. 3581.
(24) Mou, L.; Li, Z.; Qi, J.; Jiang, X. *CCS Chem.* **2021**, *3*, 1562−1572.
(25) Mou, L.; Dong, R.; Hu, B.; Li, Z.; Zhang, J.; Jiang, X. *Lab Chip* **2019**, *19*, 2750−2757.
(26) Mou, L.; Jiang, X. *Adv. Healthcare Mater.* **2017**, *6*, No. 1601403.
(27) Mou, L.; Hu, B.; Zhang, J.; Jiang, X. *Biomed. Microdevices* **2019**, *21*, No. 69.
(28) Du, P.-X.; Chou, Y.-Y.; Santos, H. M.; Keskin, B. B.; Hsieh, M.-H.; Ho, T.-S.; Wang, J.-Y.; Lin, Y.-L.; Syu, G.-D. *Anal. Chem.* **2021**, *93*, 7690−7698.
(29) Ter-Ovanesyan, D.; Gilboa, T.; Lazarovits, R.; Rosenthal, A.; Yu, X.; Li, J. Z.; Church, G. M.; Walt, D. R. *Anal. Chem.* **2021**, *93*, 5365−5370.
(30) Sun, B. R.; Zhou, A. G.; Li, X.; Yu, H.-Z. *ACS Sens.* **2021**, *6*, 1731−1744.
(31) Zhou, W.; Fu, G.; Li, X. *Anal. Chem.* **2021**, *93*, 7754−7762.
(32) Han, S.; Xu, Y.; Sun, J.; Liu, Y.; Zhao, Y.; Tao, W.; Chai, R. *Biosens. Bioelectron.* **2020**, *154*, No. 112073.
(33) Rowe, C. A.; Tender, L. M.; Feldstein, M. J.; Golden, J. P.; Scruggs, S. B.; MacCraith, B. D.; Cras, J. J.; Ligler, F. S. *Anal. Chem.* **1999**, *71*, 3846−3852.
(34) Delehanty, J. B.; Ligler, F. S. *Anal. Chem.* **2002**, *74*, 5681−5687.
(35) Ferrara, F.; Temperton, N. *Methods Protoc.* **2018**, *1*, 8.
(36) Wang, C.; Wang, C.; Qiu, J.; Gao, J.; Liu, H.; Zhang, Y.; Han, L. *Microchim. Acta* **2021**, *188*, No. 262.
(37) Wechselberger, C.; Süßner, S.; Doppler, S.; Bernhard, D. *J. Clin. Virol.* **2020**, *131*, No. 104589.
(38) Klüpfel, J.; Koros, R. C.; Dehne, K.; Ungerer, M.; Würstle, S.; Mautner, J.; Feuerherd, M.; Protzer, U.; Hayden, O.; Elsner, M.; Seidel, M. *Anal. Bioanal. Chem.* **2021**, *413*, 5619−5632.

https://doi.org/10.1021/acs.analchem.1c04383
Anal. Chem. 2022, 94, 2510−2516